Quasi- and Nonequivalence in the Structure of Bacterial Flagellar Filament

Kazuya Hasegawa,*# Ichiro Yamashita,* and Keiichi Namba*
*International Institute for Advanced Research, Matsushita Electric Industrial Company, Seika 619-02, and #Institute for Protein Research, Osaka University, Suita 565, Japan

ABSTRACT In supercoiled forms of flagellar filaments, which are thought to be produced by combinations of two distinct subunit lattices, the lattices are elastically deformed in 11 different ways, depending on their azimuthal positions on the circumference of a tube with 11 protofilaments. Those two interactions are nonequivalent as opposed to quasiequivalent ones in elastically deformed lattices of otherwise identical interactions. The term *nonequivalence* is defined to represent different bonding interactions, and *quasiequivalent* is used to describe deformed but conserved bonding interactions. By using two distinct lattices that were accurately determined by x-ray fiber diffraction, 10 possible supercoiled forms of flagellar filaments were simulated, based on a bistable-subunit packing model. Comparison to the observed forms showed good agreement, indicating that the model and determined lattice parameters effectively represent realistic features of the structure. The simulated quasiequivalent lattices have been compared to the two nonequivalent lattices, revealing an interesting feature: the maximum deviation in the intersubunit distance by elastic deformation is almost three-quarters of the difference between the two distinct lattices, demonstrating a balanced coexistence of a well-defined conformational distinction and extensive adaptability in the molecular structure of flagellin and its packing interactions.

INTRODUCTION

Bacteria swim by rotating the flagellar filaments. During the straight-swimming phase, the flagellar filaments form a bundle behind the cell body, where the filaments are all in a left-handed supercoiled form, each acting as a propeller driven by a rotary motor at the base of the filament (Berg and Anderson, 1973; Silverman and Simon, 1972; Larsen et al., 1974). Bacteria tumble frequently to change their swimming directions for taxis. The tumbling is caused by quick reversal of motor rotation, which produces a twisting torque and transforms the filaments into right-handed supercoils momentarily (Macnab and Ornston, 1977). The transformation first occurs at the base of the filament, where the largest twisting torque is produced, and it propagates to the distal end quickly. This allows the bundle to fall apart smoothly, which then makes the propelling forces uncoordinated, resulting in a rapid change of the cell's orientation. Thus the dynamic properties of the flagellar filaments play an essential role in bacterial chemotaxis. The flagellar filaments can also be transformed into various but distinct polymorphic forms, including two straight forms, in response to amino acid replacements in flagellin (Leifson, 1960; Iino and Mitani, 1966; Martinez et al., 1968; Asakura and Iino, 1972; Iino et al., 1974; Hyman and Trachtenberg, 1991; Kanto et al., 1991) and to chemical changes in the environment (Kamiya and Asakura, 1976, 1977) as well as to mechanical forces (Macnab and Ornston, 1977; Hotani, 1982).

Received for publication 15 April 1997 and in final form 30 June 1997.

Address reprint requests to Dr. Keiichi Namba, International Institute for Advanced Research, Matsushita Electric Industrial Co., 3-4 Hikaridai, Seika 619-02. Tel.: 81-774-98-2543; Fax: 81-774-98-2575; E-mail: keiichi@crl.mei.co.jp.

0006-3495/98/01/569/07 $2.00

The flagellar filament is composed of a single protein, flagellin. The filament is a tubular structure composed of 11 protofilaments, made up of nearly longitudinal arrays of subunits (O'Brien and Bennett, 1972), and is built by a self-assembly process (Asakura et al., 1964). Supercoiled forms of the filaments are thought to be constructed from a mixture of two distinct subunit lattices arranged in a regular manner (Asakura, 1970; Calladine, 1975, 1976, 1978). There are actually two types of straight flagellar filaments with distinct helical symmetries; the protofilaments are twisted into left-handed helices in one and right-handed in the other, and therefore they are called the L- and R-type, respectively (Kamiya et al., 1979). The straight filaments isolated from mutant strains SJW1660 and SJW1655, which are point mutants of a wild-type strain SJW1103 (Hyman and Trachtenberg, 1991; Kanto et al., 1991), have the helical symmetry of the L- and R-type, respectively, and these two types of flagellins can be copolymerized to form different types of supercoiled filaments, depending on the mixing ratio (Kamiya et al., 1980). Therefore, those two subunit lattices, formed by either two subunit conformations or two types of intersubunit interactions, are thought to represent the two that coexist in the supercoiled filaments (Kamiya et al., 1979, 1980).

The structures of the two types of straight filaments were deduced at ~10-Å resolution by electron cryomicroscopy and helical image reconstruction (Mimori et al., 1995; Morgan et al., 1995). The two structures show a common feature of domain arrangements of the flagellin subunit. The filaments are composed of a densely packed core region out to a radius of ~60 Å, a central channel with a diameter of ~30 Å, and well-resolved outer parts that slew out to a radius of 115 Å. There are two radial regions of high density in the core region, from 15 to 30 Å and from 35 to 60 Å, where

many rodlike features extend nearly parallel to the filament axis and are packed continuously in both axial and lateral directions. These rodlike features are interpreted as axially aligned α-helical coiled coils. The two radial regions form a concentric double-tubular structure, and the two tubes, called the inner and outer tube, are connected by radial spokelike densities. This core structure appears to play important roles in determining and stabilizing the tubular structure of the filament.

Direct comparison of the L- and R-type structures shows no significant differences in the overall structure of the subunits, and the subunit orientation is only slightly changed, in accordance with the different tilt of the protofilaments (Mimori-Kiyosue et al., 1996). The structures of straight filaments reconstituted from various types of terminally truncated flagellin fragments were also analyzed, and all of those filaments were found to have an identical symmetry that is different from either the L- or R-type (Mimori-Kiyosue et al., 1996). Its helical symmetry was named the Lt-type, where L stands for the left-handed protofilament tilt, with an angle much larger than that of the L-type, and t for truncated fragments. In the Lt-type filament, the inner-tube domain interactions are either not properly formed or are missing, and these structural defects appear to be responsible for formation of the Lt-type lattice. Again, the overall structure of the subunit is identical to those of the L- and R-type, and the subunit orientation is changed only in accordance with the different tilt angle of the protofilaments. Close comparison of the local subunit lattices of the three structures at the radius of the outer tube shows that, despite the differences in the overall symmetry of their packaging, the Lt-type lattice is almost identical to the R-type, indicating strong bistable (that is, two distinct stable) interactions between the outer-tube domains and their preference for being in the R-type in the absence of the inner-tube structure (Mimori-Kiyosue et al., 1996; Yamashita et al., manuscript submitted for publication). This also indicates that the bistable interactions between the α-helical segments in the outer tube are responsible for the polymorphic properties of the filament.

Based on a bistable-subunit model (Asakura, 1970; Calladine, 1975, 1976, 1978) and using two distinct cylindrical surface lattices at the outer-tube radius (45 Å) obtained from the structural parameters (accurately determined by x-ray fiber diffraction), the curvature and twist of 10 possible supercoiled forms have been calculated (Yamashita et al., manuscript submitted for publication). Comparison to results from electron and optical microscopy shows good agreement, indicating that the model and determined lattice parameters effectively represent realistic features of the structure (Fig. 3). In those supercoils, each strand lattice formed by two adjacent protofilaments is elastically deformed in 11 different ways, depending on the azimuthal positions of the strand lattices on the circumference of the tube. The elastically deformed lattices of otherwise identical interactions are quasiequivalently related, as opposed to the two nonequivalent interactions found in the L- and R-type filaments. The term *quasiequivalence* was defined by Caspar and Klug (1962) to describe deformed but conserved bonding interactions, and *nonequivalence* is defined to represent distinct bonding interactions, as suggested by Asakura (1970). In the present study, we have analyzed the amount of deformation in the quasiequivalent lattices of the supercoils in comparison with the difference between the two nonequivalent ones. The results show an interesting feature: the maximum deviation in the intersubunit distance from each of the two distinct states is almost three-quarters of the difference between the two, which demonstrates a balanced coexistence of a well-defined conformational distinction and extensive adaptability in the molecular structure of flagellin and its packing interactions in the filament structure.

METHODS

Calculation of the curvature and twist of supercoiled forms

Following a bistable-subunit model for the tubular structure of flagellar filaments (Calladine, 1976), which has long and short strand joints of linear-elastic properties, the curvature and twist of supercoiled forms produced by combining two lattices can be calculated as follows. The term *strand joint* is defined here as the lattice formed by two adjacent protofilaments, in the same way as the term *strand* was defined by Calladine (1975, 1976, 1978). There are two types of strand joints, namely the L- and R-type, and 11 strand joints form the tubular structure of the flagellar filament. Cylindrical surface lattices of supercoils are made by putting together the L- and R-type strand joints, so that some of the 11 strand joints are in the L-type and the rest are in the R-type. Closing of those surface lattices to form the tubular structures without misregistering the lattice disposition at the closing interface requires the protofilament tilt angle to be adjusted. Every change of one strand joint into the other state results in almost the same amount of change in the protofilament tilt angle, which determines the twist of supercoils. Therefore, the twists are almost equally separated in Fig. 3 between those of the L- and R-type. This almost equal separation comes from the fact that only a small change in the tilt angle ($\sim$0.45°) is produced by the switching of a single strand joint, and therefore the shift of the lattice points by the switching is always almost parallel to the filament axis. This results in approximately the same amount of tilt of the surface lattice for registering the lattice points at the closing interface.

The curvature of a supercoil, κ_n, can be calculated by the following equations from the repeat distances of the short (R-type) and long (L-type) strand joints, $d_{11\text{-}L}$ and $d_{11\text{-}R}$, respectively, and the number of the short strand joints, n, which varies from 0 to 11. Here the repeat distance of a strand joint is the intersubunit distance along the strand

joint. The curvature, κ_n, is obtained by

$$\kappa_n = \frac{4\delta \cdot \sin(n\pi/11)}{11 \cdot \sin(\pi/11) \cdot d \cdot 2r} \quad (1)$$

where δ is the axial component of the difference between $d_{11\text{-L}}$ and $d_{11\text{-R}}$, calculated by

$$\delta = (d_{11-L} - d_{11-R}) \cdot \cos\,\theta_n \quad (2)$$

d is the axial distance between the two cross sections of the tube that are slightly tilted to each other and connected by the 11 strand joints of the unit repeat distances, calculated by

$$d = d_{11-L} \cdot \cos\,\theta_n - n\delta/11 \quad (3)$$

and r is the radius of the tube. Here the protofilament tilt angle, θ_n, is defined relative to the filament axis in the plane of a cylindrical surface lattice at the radius of the tube, where the clockwise tilt is positive. The angle θ_n can be well approximated by the following equation, using the two protofilament tilt angles, θ_L and θ_R of the L- and R-type, respectively:

$$\theta_n = \{(11 - n) \cdot \theta_L + n \cdot \theta_R\}/11 \quad (5)$$

Equation 1 can be derived as follows. The axial component of the repeat distance of the jth strand joint that connects the two cross sections, d_j, is determined as

$$d_j = d - (2\delta/11) \cdot \sum_{k=0}^{n-1} \cos(2\pi j/11 - 2\pi k/11) \quad (6)$$

where k denotes the positions of R-type strand joints. The summation in Eq. 6 over k results in

$$d_j = d - \frac{2\delta \cdot \sin(n\pi/11)}{11 \cdot \sin(\pi/11)} \cdot \cos\{2\pi j/11 - (n-1)\pi/11\} \quad (7)$$

The curvature of a supercoil, κ_n, can be calculated from δ', the difference between the minimum and maximum of d_j obtained by treating j in Eq. 7 as a real number to find the distances along the innermost and outermost lines of the supercoiled tube. Treating j as a real number is necessary because one of these two lines is always between strand joints. From Eq. 7, δ' is obtained as

$$\delta' = \frac{4\delta \cdot \sin(n\pi/11)}{11 \cdot \sin(\pi/11)} \quad (8)$$

Finally, the radius of the curvature, $1/\kappa_n$, can be obtained as the distance between the tube axis and the intersection of the extended planes of the two cross sections of the tube, where these two lines are perpendicular to each other. The ratio of this distance to the axial distance between the two cross sections, d, is the same as the ratio of the tube diameter, $2r$, to δ', and therefore $1/\kappa_n$ is obtained by

$$\frac{1}{\kappa_n} = \frac{d \cdot 2r}{\delta'} \quad (9)$$

Thus Eq. 1 can be derived from Eqs. 8 and 9.

The protofilament tilt angles of the L- and R-type straight filament, θ_L and θ_R in Eq. 5, defined on the cylindrical surface at the radius r, are calculated from the twist, τ_L and τ_R, of those two filaments, respectively, for example, by

$$\theta_L = \tan^{-1}(r \cdot \tau_L) \quad (10)$$

The twist of a supercoil, τ_n, can be also calculated by Eq. 10 from θ_n in Eq. 5. The values used for τ_L and τ_R are -5.62 and 13.44 rad/μm, respectively, as shown in Fig. 3. The distances used for $d_{11\text{-L}}$ and $d_{11\text{-R}}$ are 52.7 and 51.9 Å, respectively. Those values were obtained by x-ray measurements by Yamashita et al. (manuscript submitted for publication). The tube radius, r, is 45 Å, which is the outer-tube radius of the filament.

Model building

Once the curvature κ_n and twist τ_n are determined as above for 10 supercoils composed of n R-type strand joints and $11 - n$ L-type strand joints, where n is 1–10, models of the supercoils and two straight filaments are constructed by putting rectangular tiles 25 Å wide and 50 Å long on the surface of the outer tube. The rectangular tiles represent α-helical coiled coils that are oriented with their long axes along the protofilaments.

The pitch, P, and radius, R, of a supercoil are calculated by the following two equations:

$$P = 2\pi\tau_n/(\tau_n^2 + \kappa_n^2) \quad (11)$$

$$R = \kappa_n/(\tau_n^2 + \kappa_n^2) \quad (12)$$

The contour line of the supercoil is defined by these values. The local lattice of the cylindrical surface of the supercoil can be produced by putting together $11 - n$ L-type and n R-type lattices, keeping the local subunit arrangements of the L- and R-type lattices unchanged. This local surface lattice is transformed into the surface lattice of the supercoil by transforming the straight z axis of the former into the helical contour line of the supercoil. The coordinates of four corner points of rectangular plane tiles are calculated according to the produced lattice, and the solid surface of the tiles is colored and shaded to produce the models shown in Fig. 2. The graphic representation of the models was done using a Silicon Graphics workstation with OpenGL graphic library routines.

RESULTS AND DISCUSSION

Polymorphic model

Fig. 1 is a reproduction of a model by Namba and Vonderviszt (1997), which describes a plausible switching of the subunit interactions involved in flagellar polymorphism. Numbered units represent outer-tube domains of flagellin subunits comprising α-helical coiled coils that are aligned roughly parallel to the filament axis and packed closely in all directions. In this model the subunits do not show any conformational switching, but only the subunit packing mode switches between the L- and R-type lattice, as inferred from the structural information on the two types of straight filaments, revealed by x-ray fiber diffraction (Namba et al., 1989; Yamashita et al., manuscript submitted for publication) and electron cryomicroscopy (Mimori et al., 1995; Morgan et al., 1995; Mimori-Kiyosue et al., 1996). According to this model, 12 possible polymorphic forms of the flagellar filaments are drawn in Fig. 2 as tubular structures formed by rectangular blocks that represent the outer-tube domains. The diameter of the tube is 90 Å, and the size of each rectangular block is ~50 Å by 25 Å. Each of 11 interfaces of two adjacent protofilaments is colored either blue or red. When the lattice formed by two adjacent protofilaments is the L-type, the interface is colored blue; when the lattice is the R-type, the interface is colored red.

The curvatures and twists of those model tubes shown in Fig. 2 were calculated by the equations and structural parameters given above, and they were compared with ob-

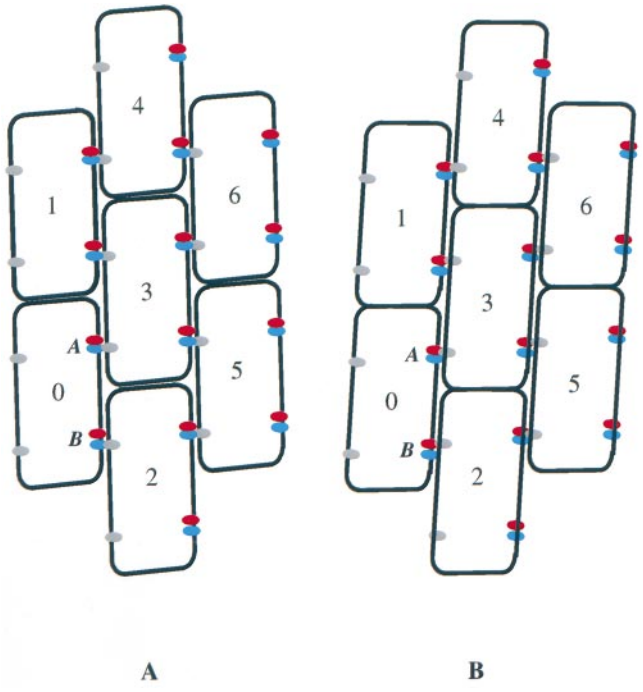

FIGURE 1 A plausible model of switching involved in flagellar polymorphism. (*A*) Subunit packing in the L-type. (*B*) Subunit packing in the R-type. The filament axis is vertical. The model represents the subunit interactions in the outer tube. The elongated building blocks represent α-helical bundles aligned nearly parallel to the filament axis. Subunits are numbered accordingly in *A* and *B*. Two hypothetical binding regions of the subunits are labeled *A* and *B*, where the blue-gray interaction represents the L-type packing and the red-gray interaction represents the R-type. The distances between the red and blue sites are 1.8 Å for the *A* region and 2.6 Å for the *B* region, which makes the intersubunit distance along the protofilament (between subunits 0 and 1) 0.8 Å longer in the L-type than that in the R-type, as observed. The only essential feature of the binding sites is the two discrete relative dispositions, and any alternative bonding arrangements that fulfill this feature would be satisfactory.

served values (Yamashita et al., manuscript submitted for publication), which is reproduced in Fig. 3. For this calculation, the essential features of the model are the two distinct lattices and linear-elastic properties of the protofilaments in the structural deformation when they form supercoils, as described by Asakura (1970) and Calladine (1975, 1976, 1978). The comparison shows good agreement, indicating that the model represents the essential features of flagellar polymorphism and that the two distinct structural parameters obtained by experimental measurements are quantitatively sound.

Here the important values are the two distinct intersubunit distances along the protofilaments, 52.7 Å and 51.9 Å for the L- and R-type, respectively. The small difference between the two, namely 0.8 Å, is responsible for the curvatures of the filaments shown in Fig. 3. In the model of Fig. 1, the switching is represented as mutual sliding of the rectangular blocks along the protofilament interface by two distinct short distances. The two distances are 1.8 and 2.6 Å at two different interface sites, namely sites *A* and *B* in Fig. 1, respectively. The difference between these two distances produces a change in the intersubunit distance of 0.8 Å. These two distances, or at least the larger one, 2.6 Å, is thought to be somehow related to the pitch of the α-helix, because the switching appears to be mutual sliding between α-helical coiled coils over one turn of the α-helix with some adjustment of side-chain interactions, although no direct experimental evidence has been obtained yet.

Quasiequivalence and nonequivalence

Although the difference between the two types of subunit packing is very small as described above, the distinction between the two appears to be well defined. Therefore, the two states can be called nonequivalent states, where different bonding interactions are likely to be involved. On the other hand, in supercoiled forms, the repeat distances of the 11 strand joints are all different from either of the two states; the lengths are not only different between the protofilaments in the two different states, but also different even within a group of identical states. The differences are caused by elastic deformations, which are necessary to form a closed tubular structure with 11 strand joints having two distinct repeat distances and lateral dispositions. Strand joints of an identical state but different repeat distances can be called quasiequivalent.

These differences are due to the stretch or compression of strand joints caused by the long- and short-type strand joints on the circumference of the tube. Although the free energy is increased by having two different intersubunit interactions and elastic strains produced by those changes in the repeat distances of strand joints, a relatively large negative energy is gained by bonding the protofilament interfaces to close the tubular structure. Thus the free energy of the whole system is decreased by forming the tubular filament of supercoiled forms.

As discussed by Namba and Vonderviszt (1997), it appears from the structure of the filament that the relative disposition between the inner-tube and outer-tube domain interactions is designed to define the protofilament tilt somewhere between those of the L- and R-type, and at a given tilt angle the tube cannot be closed without misfitting the protofilament interface if all of the strand joints are in one of the two lattices. It is possible to close the tube only by having some number of the R-type strand joints as well as the L-type ones, which results in a particular curvature and twist, which in turn create a supercoil with a particular pitch and diameter. Thus quasiequivalent states are a feature of the molecular design of the flagellar filament that is essential for forming supercoils.

We have analyzed the quasiequivalent states in various supercoils to estimate how large a deformation is allowed in the structure without having one state turn into the other. For each supercoiled form simulated in Fig. 2, which has a curvature and twist given in Fig. 3, the repeat distances of the 11 strand joints are plotted in Fig. 4, with the type of each strand joint identified by either blue (L-type) or red

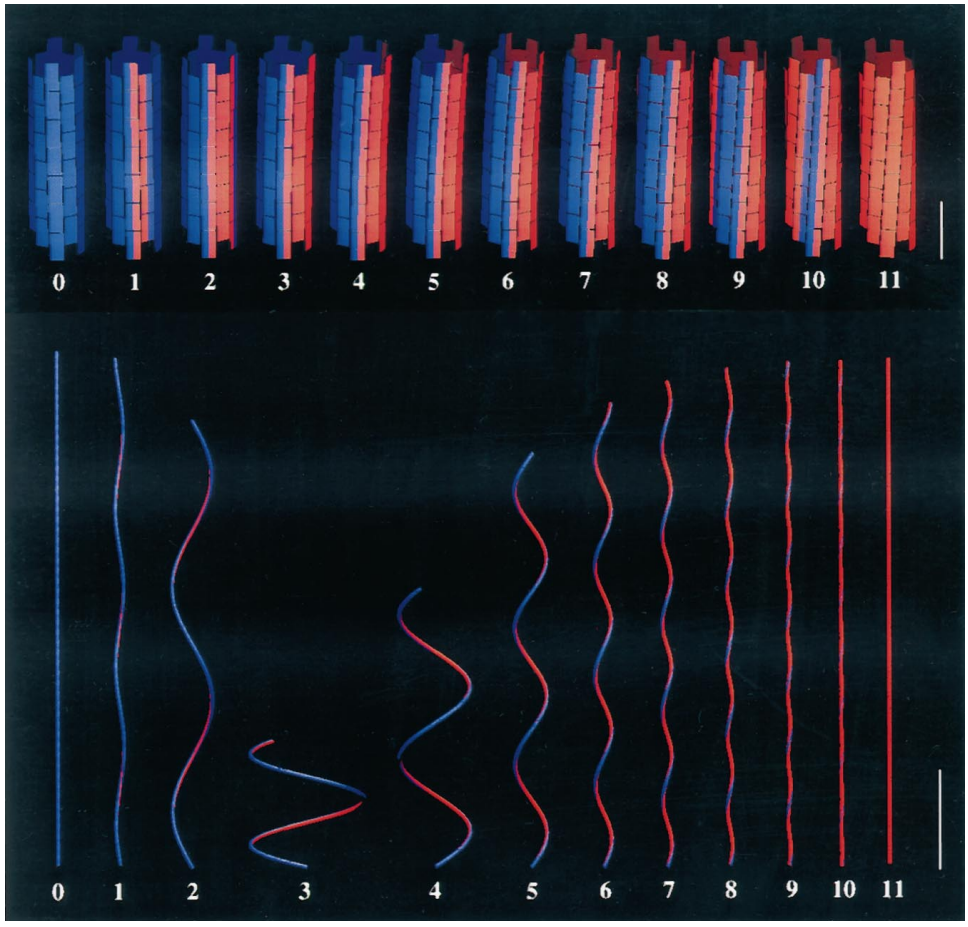

FIGURE 2 Polymorphic model of flagellar filament. Short (*A*) and long (*B*) segments of the tubular structures are drawn for the L- and R-type straight filaments at the extreme left and right, respectively, and for 10 supercoils between the two. The tubes shown in *A* represent the outer-tube lattices at a diameter of 90 Å, where rectangular tiles represent outer-tube domains of flagellin subunits, just as shown in Fig. 1. Colors around the protofilament interface indicate the type of lattice formed by two adjacent protofilaments (strand joint): blue, the L-type; red, the R-type. The diameter of the long filaments in *B* is 400 Å, to display a certain thickness of the filaments with colors of the L- and R-type strand joints on the outer and inner sides of the supercoiled tubes, respectively. The numbers below the models indicate the number of the R-type strand joints, *n*, used in the equations in Methods. The short segments in *A* are composed of 70 tiles, for which the scale bar is 100 Å. The long filaments in *B* are composed of 10,680 tiles, which produce exactly two turns of normal filament ($n = 2$). The three-dimensional coordinates of the tiles are calculated by the procedure described in Methods. The pitch and radius of the filaments in *B* are listed in Table 1. Scale bar, 1 μm.

TABLE 1 The pitch and radius of the supercoil models shown in Fig. 2

n	1	2	3	4	5	6	7	8	9	10
P	1.576	2.233	0.901	1.429	1.361	1.087	0.881	0.733	0.621	0.535
R	0.040	0.196	0.563	0.350	0.156	0.080	0.044	0.024	0.012	0.005
N_S	303	485	696	500	321	229	177	144	120	103

The number of the R-type strand joints in each supercoil is listed as *n*. The pitch, *P*, and radius, *R*, of each supercoil are calculated from its curvature and twist by Eqs. 11 and 12, and are listed in μm. The curvature and twist are calculated by Eqs. 1 and 10, respectively, from the two twists and intersubunit distances along the protofilament obtained for the L- and R-type lattices. The number of subunits in the length of a protofilament in one turn of the supercoil is listed as N_S. The range of the lengths and total numbers of subunits in typical flagellar filament are from 10 to 15 μm and from 21,000 to 32,000, respectively.

(R-type). Because the strand joints of an identical-type cluster on one side of the tube for minimizing the strain energy over the whole filament, all of the R-type (short) strand joints have shorter repeat distances than any of the L-type (long) strand joints. However, the deformations reach up to 0.6 Å, which is almost three-quarters of the difference between the two states, 0.8 Å. This indicates that flagellin molecules have relatively high conformational flexibility and adaptability in either of the states, while having two well-defined and distinct states of subunit interactions.

Quasiequivalence is found not only in the lengthwise deformation, but also in the twisting deformation of the protofilaments. Although the protofilament helix is left-handed in the L-type filament and right-handed in the R-type, the protofilaments of supercoils can be left- or right-handed regardless of the type of strand joints they form, as indicated in the models shown in Fig. 2 and by the protofilament twist in Fig. 3. This means that the protofilaments can be twisted in both directions regardless of the conformational state. A much clearer example is found in the structure of the Lt-type filaments, which are reconstituted from terminally truncated flagellin fragments (Mimori-Kiyosue et al., 1996). The protofilament of the Lt-type filament has a left-handed twist, but much greater than that of the L-type filament, and yet the local subunit interactions including the repeat distance of the strand joint are almost identical to those of the R-type. This is possible because the

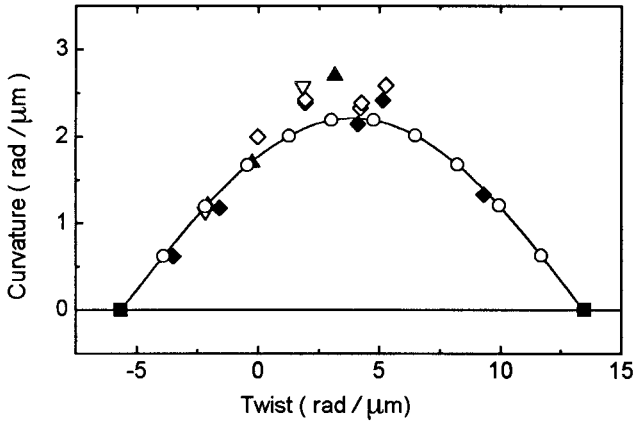

FIGURE 3 Curvature and twist of polymorphic forms of flagellar filaments. The curvatures and twists of 10 forms of supercoils shown in Fig. 2 were calculated and plotted (–○–). The two solid squares with zero curvature represent the two straight filaments: the L-type on the left and the R-type on the right. Other symbols are for curvatures and twists calculated from pitches and diameters of various supercoiled filaments observed by optical microscopy: ▲, SJ670 (Kamiya and Asakura, 1976); ▽, SJ25 (Kamiya and Asakura, 1976); ♦, copolymer of SJW1655 and SJW1660 (Kamiya et al., 1980); ◇, copolymer of SJW1655 and SJW1658 (Kamiya et al., 1980). This is a partial reproduction of a figure to be presented in a original work by Yamashita et al. (manuscript submitted for publication).

Lt-type lattice is related to the R-type lattice by a reconstructive transformation, which involves breaking the bonds at a protofilament interface, mutual translation of protofilaments at the interface by one subunit, and closing the interface. This transformation requires a relatively large amount of twisting of the outer tube without changing the local arrangement of the cylindrical surface lattice of the R-type. If the outer-tube domain were a thin rigid tile with a size of ~25 Å by 50 Å, the twisting deformation of the outer tube would produce the maximum shearing of 2.4 Å at the domain interface. This shearing, however, must be adjusted by the flexibility and adaptability of flagellin subunits to conserve the bonding interactions. Thus the outer tube structure also has a large flexibility and adaptability in the twisting deformation to be in a wide range of quasiequivalent states, so that the outer tube is able to form stable supercoils.

As a result of the large amount of left-handed twist in the outer tube of the Lt-type compared to that of the R-type, the inner-tube lattice becomes largely deformed. This is most likely to be related to the absence of the inner-tube structure in the Lt-type filament, indicating that proper interaction between the terminal regions in the intact-filament lattice is essential to construction of the inner-tube structure. This also means that in intact filaments the mutual dispositions of the inner- and outer-tube domain interactions determine the twist of the protofilaments within a range defined by the L- and R-type structures, which in turn determines the number of the L- and R-type protofilament lattices to be mixed to form a tubular structure without a mismatch at the protofilament interfaces, which as a result determines that the filament structure will be a particular form of supercoil. It is also important to note that the local lattice of the inner tube remains virtually invariant, even when the outer tube connections are switched between the L- and R-type lattices, which suggests that the inner-tube interactions may not necessarily be involved in the same nonequivalent switching as the outer-tube ones and that there may be only quasiequivalent deformations in the inner tube. This appears to be a plausible mechanism of flagellar polymorphism.

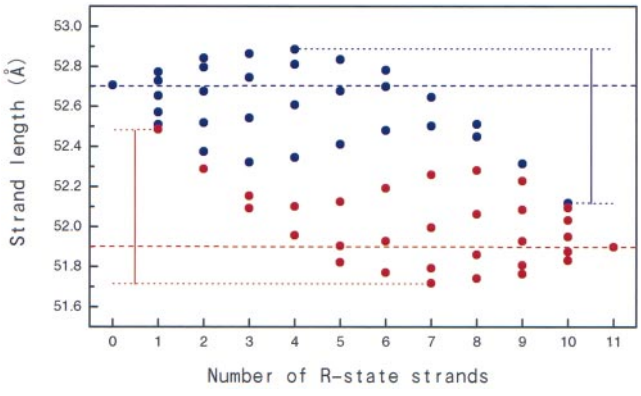

FIGURE 4 Intersubunit distances along the 11 strand joints in 10 forms of supercoils and two straight forms. Blue circles represent those of the L-type strand joints; red circles those of the R-type strand joints. The blue and red circles at the extreme left and right, respectively, are for the straight filament of the L-type ($n = 0$) and R-type ($n = 11$), respectively. For these straight filaments, the repeat distances of the 11 strand joints are all the same, and therefore there is only one circle for each located on the broken line with the same color. The ranges of variation are indicated with vertical solid lines: blue, the L-state strand joint; red, the R-state strand joint. The maximum deviations from the resting states within the same type of strand joints are almost three-quarters of the difference between the L- and R-type strand joints, demonstrating the flexibility and adaptability of the tubular structure of the flagellar filament.

We gratefully acknowledge the continuous interest in, and critical comments and discussion on our work by D. L. D. Caspar and S. Asakura, who put forward the concepts of quasi- and nonequivalence, respectively. We dedicate this paper to both of them. We also thank F. Oosawa, T. Tsukihara, and T. Nitta for their support and encouragement.

This work was supported in part by Special Coordination Funds of the Science and Technology Agency of Japan to KN.

REFERENCES

Asakura, S. 1970. Polymerization of flagellin and polymorphism of flagella. *Adv. Biophys.* 1:99–155.

Asakura, S., G. Eguchi, and T. Iino. 1964. Reconstitution of bacterial flagella in vitro. *J. Mol. Biol.* 10:42–56.

Asakura, S., and T. Iino. 1972. Polymorphism of *Salmonella* flagella as investigated by means of in vitro copolymerization of flagellins derived from various strains. *J. Mol. Biol.* 4:251–268.

Berg, H. C., and R. A. Anderson. 1973. Bacteria swim by rotating their flagellar filaments. *Nature.* 245:380–382.

Calladine, C. R. 1975. Construction of bacterial flagella. *Nature.* 225: 121–124.

Calladine, C. R. 1976. Design requirements for the construction of bacterial flagella. *J. Theor. Biol.* 57:469–489.

Calladine, C. R. 1978. Change of waveform in bacterial flagella: the role of mechanics at the molecular level. *J. Mol. Biol.* 118:457–479.

Caspar, D. L. D., and A. Klug. 1962. Physical principles in the construction of regular viruses. *Cold Spring Harb. Symp. Quant. Biol.* 27:1–24.

Hotani, H. 1982. Micro-video study of moving bacterial flagellar filaments. III. Cyclic transformation induced by mechanical force. *J. Mol. Biol.* 156:791–806.

Hyman, H. C., and S. Trachtenberg. 1991. Point mutations that lock *Salmonella typhimurium* flagellar filaments in the straight right-handed and left-handed form and their relationship to filament superhelicity. *J. Mol. Biol.* 220:79–88.

Iino, T., and M. Mitani. 1966. Flagella-shape mutants in *Salmonella*. *J. Gen. Microbiol.* 44:27–40.

Iino, T., T. Oguchi, and T. Kuroiwa. 1974. Polymerization in flagellar-shape mutants of *Salmonella typhimurium*. *J. Gen. Microbiol.* 81:37–45.

Kamiya, R., and S. Asakura. 1976. Helical transformations of *Salmonella* flagella in vitro. *J. Mol. Biol.* 106:167–186.

Kamiya, R., and S. Asakura. 1977. Flagellar transformations at alkaline pH. *J. Mol. Biol.* 108:513–518.

Kamiya, R., S. Asakura, K. Wakabayashi, and K. Namba. 1979. Transition of bacterial flagella from helical to straight forms with different subunit arrangements. *J. Mol. Biol.* 131:725–742.

Kamiya, R., S. Asakura, and S. Yamaguchi. 1980. Formation of helical filaments by copolymerization of two types of "straight" flagellins. *Nature.* 286:628–630.

Kanto, S., H. Okino, S.-I. Aizawa, and S. Yamaguchi. 1991. Amino acids responsible for flagellar shape are distributed in terminal regions of flagellin. *J. Mol. Biol.* 219:471–480.

Larsen, S. H., R. W. Reader, E. N. Kort, W. W. Tso, and J. Adler. 1974. Change in direction of flagellar rotation is the basis of the chemotactic response in *Escherichia coli*. *Nature.* 249:74–77.

Leifson, E. 1960. Atlas of Bacterial Flagellation. Academic Press, New York and London.

Macnab, R. M., and M. K. Ornston. 1977. Normal-to-curly flagellar transitions and their role in bacterial tumbling. Stabilization of an alternative quaternary structure by mechanical force. *J. Mol. Biol.* 112: 1–30.

Martinez, R. J., A. T. Ichiki, N. P. Lundh, and S. R. Tronick. 1968. Single amino acid substitution responsible for altered flagellar morphology. *J. Mol. Biol.* 34:559–564.

Mimori, Y., I. Yamashita, K. Murata, Y. Fujiyoshi, K. Yonekura, C. Toyoshima, and K. Namba. 1995. The structure of the R-type straight flagellar filament of *Salmonella* at 9 Å resolution by electron cryomicroscopy. *J. Mol. Biol.* 249:69–87.

Mimori-Kiyosue, Y., F. Vonderviszt, I. Yamashita, Y. Fujiyoshi, and K. Namba. 1996. Direct interaction of flagellin termini essential for polymorphic ability of flagellar filament. *Proc. Natl. Acad. Sci. USA.* 93: 15108–15113.

Morgan, D. G., C. Owen, L. A. Melanson, and D. J. DeRosier. 1995. Structure of bacterial flagellar filaments at 11 Å resolution: packing of the α-helices. *J. Mol. Biol.* 249:88–110.

Namba, K., and F. Vonderviszt. 1997. Molecular architecture of bacterial flagellum. *Q. Rev. Biophys.* 30:1–65.

Namba, K., I. Yamashita, and F. Vonderviszt. 1989. Structure of the core and central channel of bacterial flagella. *Nature.* 342:648–654.

O'Brien, E. J., and P. M. Bennett. 1972. Structure of straight flagella from a mutant *Salmonella*. *J. Mol. Biol.* 70:133–152.

Silverman, M., and M. Simon. 1972. Flagellar assembly mutants in *Escherichia coli*. *J. Bacteriol.* 112:986–993.